Check for updates

THE AMERICAN SOCIETY OF MECHANICAL ENGINEERS
345 E. 47th St., New York, N.Y. 10017

97-GT-73

The Society shall not be responsible for statements or opinions advanced in papers or discussion at meetings of the Society or of its Divisions or Sections, or printed in its publications. Discussion is printed only if the paper is published in an ASME Journal. Authorization to photocopy material for internal or personal use under circumstance not falling within the fair use provisions of the Copyright Act is granted by ASME to libraries and other users registered with the Copyright Clearance Center (CCC) Transactional Reporting Service provided that the base fee of $0.30 per page is paid directly to the CCC, 27 Congress Street, Salem MA 01970. Requests for special permission or bulk reproduction should be addressed to the ASME Technical Publishing Department.

Copyright © 1997 by ASME All Rights Reserved Printed in U.S.A

Downloaded from http://asmedigitalcollection.asme.org/GT/proceedings-pdf/GT1997/78699/V002T06A008/2409092/v002t06a008-97-gt-073.pdf by guest on 02 December 2022

# QUANTIFYING UNMIXEDNESS IN LEAN PREMIXED COMBUSTORS OPERATING AT HIGH PRESSURE, FIRED CONDITIONS

**J.C. Barnes and A.M. Mellor**
**Vanderbilt University, Nashville, TN 37235**

BREAK

## ABSTRACT

Lean premixed combustor manufacturers require premixer concepts that provide homogeneity (mixedness) of the fuel which burns in the main flame. Ideally premixer evaluation would be conducted under realistic combustor operating conditions. However, current techniques typically are limited to cold–flow, low pressure (<14 atm) conditions or comparison of measured $NO_x$ emissions with others obtained in premixed systems. Thus, a simple, consistent method for quantifying unmixedness in lean premixed combustors operating at high pressure, fired operating conditions is proposed here, using the characteristic time model developed in the companion paper.

## INTRODUCTION

Lean premixed (LP) combustion is a technique for pollutant emissions control which is seeing increased application in gas turbines as an alternative to conventional, diffusion flame combustion. In the low emissions mode, an ideal combustor of this type produces a homogeneous, lean fuel and air mixture and thereby eliminates the stoichiometric eddies found in conventional, diffusion flame combustors. However, it is usually the case in LP combustors that the fuel and air are not perfectly premixed. Therefore, emissions from LP combustors (e.g., see Rasdan et al., 1994; Joshi et al., 1994; Snyder et al., 1994a; Fric, 1993) are not as low as experiments such as the well–controlled, "perfectly premixed" flameholder experiments (e.g., see Leonard and Stegmaier, 1994) indicate that they could be.

In order to perform testing of candidate premixer designs, an accurate, reliable method of quantifying fuel/air mixedness in the premixer is required. Here, following a review of current techniques for evaluating fuel/air mixing in LP combustors, a technique for deducing unmixedness from combustor emissions measurements is proposed.

## CURRENT TECHNIQUES FOR EVALUATING MIXEDNESS

### Computational Fluid Dynamics

Computational fluid dynamics (CFD) codes have been used to predict the extent of fuel/air mixing in a premixer module. Typically, the three–dimensional Reynolds–averaged forms of the mass, momentum, energy, and species conservation equations are solved along with the two equation $k$–$\epsilon$ model (see e.g. Jones and Launder, 1972) assuming non–reacting flow. Initial conditions required in a gaseous fuel/air premixer model include air and fuel flow parameters and properties, and premixer geometry.

Hautman et al. (1991) compared CFD predictions to experimental measurements of jet penetration and local mass fraction for a single transverse nitrogen jet injected into subsonic air flow in a rectangular test section. Quarts windows on the side and top of the test section allowed optical access. The mass distribution of the injected gas was determined via

Presented at the International Gas Turbine & Aeroengine Congress & Exhibition
Orlando, Florida — June 2–June 5, 1997

Mie scattering from titanium dioxide particles (diameter 1 $\mu$m) seeded into the gas injection stream. In general, Hautman et al. (1991) report that the CFD analysis predicted trends in jet penetration and spreading relatively well; however, the CFD significantly overpredicted the decay of maximum fuel mass fraction with downstream distance. Therefore, for the simple case of a single gaseous jet penetrating into a transverse airflow, these results indicate that CFD can only qualitatively predict fuel/air mixing. One must assume that quantitative CFD results would not improve in the case of modeling multiple fuel jets penetrating at various oblique angles into swirling air flow. Furthermore, in the case of modeling liquid fuel prevaporising premixers, where initial conditions such as the droplet number, size distribution, and time mean and rms velocity vectors associated with each droplet must be estimated, only qualitative representations of liquid fuel premixing can be expected from CFD analysis (e.g., see Snyder et al., 1994b).

Currently, for the purposes of evaluating mixedness in gaseous premixers and liquid fuel prevaporising premixers, only experimental diagnostic techniques can provide quantitative estimations of fuel/air mixing. It may also be possible to use such data to calibrate empirical expressions which could be used in the design process to calculate mixedness for a given configuration. Nevertheless, the fundamental investigation of fuel/air unmixedness effects begins with experimental measurements under practical test conditions. Techniques for measuring unmixedness experimentally are reviewed next.

Tracer Gas Measurements

Razdan et al. (1994) measured the performance of two premixer configurations. The premixers were tested in an atmospheric pressure, cold flow rig. In these tests, a tracer gas consisting of a known mixture of natural gas and air was injected through the fuel holes, and localised samples of fuel/air mixture were collected with a traversing probe. The measured local mole fraction (C) of tracer gas was normalised by the mole fraction computed assuming perfect premixing of the total metered fuel/air flow through the premixer cup ($C_{avg}$). Measurements were made at various radii and asimuthal positions in the premixer exit plane. The standard deviation in the fuel/air measurements for Configuration 1 was about 12% of $C_{avg}$, while for Configuration 2 it was about 5.5% of $C_{avg}$. Perfect premixing would correspond to a standard deviation of zero.

The types of measurements described above can be used to compute local mixedness at different axial, radial, and circumferential positions in or at the exit of the premixer cup; however, probe measurements perturb the premixer flow, are susceptible to vibrations which can lead to spatial averaging of the measurements, and generally cannot resolve temporal fluctuations in mixedness. Optical techniques have been developed to circumvent the above–mentioned shortcomings of probe measurements.

Optical Techniques

Gulati and Warren (1994) extended the work of Agarwal et al. (1976) to measure fuel/air mixing via $NO_2$ laser–induced fluorescence (LIF) in moderate pressure (less than 15 atm), cold flow systems. In this technique, natural gas fuel is simulated by nitrogen seeded with $NO_2$. Nitrogen is used instead of methane to enhance LIF signal strength and linearity. Fric (1993) used the $NO_2$ LIF technique to measure atmospheric, cold–flow fuel/air mixing. LIF measurements were sampled at a rate of approximately 20 kHz; thus spatial and temporal variations in local fuel/air concentration were measured.

Gulati and Warren (1994) note that some disadvantages associated with the $NO_2$ LIF method are 1) because of dissociation of $NO_2$ at high temperatures, the LIF technique can only be used in cold flow at temperatures less than 500 K, 2) the $NO_2$ LIF cannot be used at pressure greater than 15 atm, and 3) $NO_2$ is toxic, and extreme precautions are required during testing. Another optical method for measuring mixedness is the cold flow, Mie scattering technique of Hautman et al. (1991) described above. This technique can be considered as essentially non–intrusive since the length scale of the seed particles is less than the Kolmogorov scale of turbulence in the experimental flow. Mongia et al. (1996) discuss the development and validation (at pressures up to 10 atm in cold $CH_4$/air flow) of an inexpensive optical probe technique which measures fuel concentration directly via He–Ne laser absorption. Spatial resolution considerations require use of fiber optics, so this method is intrusive. To summarise, the current techniques discussed above for measuring mixedness are generally not capable of use during combustor testing, and it is not immediately clear how to relate these cold flow measurements of mixedness to the global performance of a combustor at fired, high pressure (typically >14 atm), high inlet temperature (~ 700 K) operating



Downloaded from http://asmedigitalcollection.asme.org/GT/proceedings-pdf/GT1997/78699/V002T06A008/2409092/v002t06a008-97-gt-073.pdf by guest on 02 December 2022

conditions.

For the purposes of premixer testing and modification, it is desirable to develop a simple, consistent method of quantifying fuel/air mixedness under realistic combustor operating conditions. Therefore, an alternative method of determining mixedness with the combustor fired is discussed next.

## ESTIMATION OF UNMIXEDNESS FROM $NO_x$ MEASUREMENTS

If it is assumed that LP $NO_x$ emissions index (g $NO_2$/kg fuel) can be expressed in terms of a global fluid mechanic time ($\tau_{sl,tno}$) and chemical kinetic time ($\tau_{tno}$) as follows (see Barnes and Mellor, 1997):

$$NO_xEI = m\big|_{\phi<1}(\tau_{sl,tno}/\tau_{tno}) \quad (1)$$

where m is a constant determined by linear regression analysis of a given set of experimental data, then for a given datum set in which the global fluid mechanic time for LP $NO_x$ is the only independent variable at a given LP flame temperature ($T_{\phi,m}$):

$$NO_xEI/\tau_{sl,tno}\big|_{T_{\phi,m}} \propto I/\tau_{tno}\big|_{T_{\phi,m}} = \text{constant}\big|_{T_{\phi,m}} \quad (2)$$

The above constraint should he satisfied for the data[1] shown in Fig. 1 in which the fluid mechanic time is the only variable (due to the difference in air flow rate hetween the two datum series) at a given flame temperature. However, the Combustor A data in Fig. 1 do not satisfy Eq. (2).

One possible interpretation of this is that the level of unmixedness, which is not accounted for in Eq. (2), is a variable between the two datum sets shown in Fig. 1 (i.e., the LP $\tau_{res}$ I data have the shorter residence time and thus the higher rms velocity in the premixer and higher mixedness). As discussed in Barnes and Mellor (1997), if the main fuel and air mixture is not homogeneous, then a distribution of equivalence ratios exists in the LP flame. Following Mikus and Heywood (1971) and Fletcher and Heywood (1971), it is assumed that this equivalence ratio distribution is Gaussian and is centered about the equivalence ratio computed assuming perfect premixing of the main fuel and air. Therefore, the form of the probahility density function (PDF) for eddies in the LP flame is:

$$\Psi(\phi_{eddy}) = \frac{1}{s\overline{\phi}_m\sqrt{2\pi}}\exp\left[\frac{-(\phi_{eddy}/\overline{\phi}_m - 1)^2}{2s^2}\right] \quad (3)$$

Here $\overline{\phi}_m$ is the mean and $\phi_{eddy}$ the local equivalence ratio associated with an individual reacting eddy. The time–averaged standard deviation in equivalence ratio in the LP flame is $\sigma_\phi$ so that

$$s \equiv \sigma_\phi/\overline{\phi}_m \quad (4)$$

following Mikus and Heywood. A standard deviation of sero corresponds to the perfectly premixed case in which all eddies in the LP flame burn with the mean equivalence ratio. Individual eddy equivalence ratios ($\phi_{eddy}$) which are greater than the mean lead to increased $NO_x$ emissions via the exponential decrease in the NO formation time with increasing eddy flame temperature.

Applying Eq. (3) to Eq. (1) one has:

$$NO_xEI\big|_{s=m}\big|_{\phi<1}\int_0^{1.4}\frac{\Psi(\phi_{eddy})\,\tau_{sl,tno}}{\tau_{tno}(\phi_{eddy})}d\phi_{eddy} \quad (5)$$

The integrand represents NO formation in an individual eddy in the LP flame with an equivalence ratio of $\phi_{eddy}$. Equation (5) reduces to Eq. (1) when s approaches sero. The lower integration limit matches the lower limit of equivalence ratio, and for nominal combustor operating conditions, the upper integration limit of 1.4 is sufficient to capture greater than 99% of the integral over the range $\pm\infty$ (see Barnes and Mellor, 1997).

In order to estimate the level of unmixedness in the LP Base 1 data, it is assumed that the LP $\tau_{res}$ 1 data correspond to perfectly premixed operating conditions ($s = 0$). Equation (1) is calibrated such that it fits the LP $\tau_{res}$ 1 data (Fig. 2). Next, the perfectly premixed model for the LP $\tau_{res}$ 1 data is modified following Eq. (5) by increasing s such that the Base 1 data are correlated. As shown in Fig. 2, this process reveals that s is on the order of 0.35 for the LP Base I data. Note that for premixed flame temperature greater than approximately 2000 K, the model predicts the sensitivity of $NO_x$ to temperature to decrease with increasing temperature). This occurs as the fraction of the eddies with $\phi_{eddy}$ greater than one increases with increasing mean equivalence ratio thus leading to lower local flame

[1]The data were collected from a gas–fired, can–type, LP gas turbine combustor, Combustor A, at constant inlet temperature and pressure. See Barnes et al. (1996) and Barnes and Mellor (1997) for a more detailed discussion of the experimental combustor data and the experimental setup used in their collection. For the full set of data, $8 \leq p_{in} \leq 14$ atm, $550 \leq T_{in} \leq 750$ K, $\tau_{res} = 13$ or 23 ms, and $0.5 \leq \phi \leq 0.8$.



Downloaded from http://asmedigitalcollection.asme.org/GT/proceedings-pdf/GT1997/78699/V002T06A008/2409092/v002t06a008-97-gt-073.pdf by guest on 02 December 2022

temperatures. Magruder et al. (1995) note that the same trend is apparent in the high temperature (>2000 K) LP $NO_x$ data of Roffe and Venkataramani (1978a).

The technique of estimating unmixedness discussed above is similar to another technique which is often used where LP $NO_x$ measurements are compared to the "perfectly premixed" data of Leonard and Stegmaier (1994). This technique is illustrated in Fig. 3. Here, the best fit of the Leonard and Stegmaier data is taken as the perfectly premixed ($s = 0$) baseline. As in the method in Fig. 2, a distribution in equivalence ratio is assumed such that the baseline model with s greater than sero correlates the experimental data of concern. Increasing values of s used to correlate the experimental data correspond to increasing unmixedness and larger displacements between the Leonard and Stegmaier data and the experimental data in question.

Using the above techniques, estimates of unmixedness can be deduced from experimental $NO_x$ data. However, some ambiguities exist with these two methods. In the case of the analysis in Fig. 2, it is unlikely that the LP $\tau_{res}$ 1 baseline data are perfectly premixed. Therefore, 0.35 is at best an estimate of the relative difference in s, and the absolute values of s cannot be computed. In the case of the analysis shown in Fig. 3, Leonard and Stegmaier report that their $NO_x$ data are independent of combustor inlet pressure and temperature, probe position, and premixer geometry. In theory, these trends may be true for gas–fired, perfectly premixed combustors, but they are certainly not true for gas–fired, practical LP combustors (see Barnes et al., 1996). Therefore, in the analysis shown in Fig. 3, the distance between the baseline and any of the experimental data trendlines is a function not only of unmixedness, but also combustor inlet temperature and pressure, residence time, and combustor geometry. Accordingly, it is difficult to make an accurate estimate of unmixedness using the technique shown in Fig. 3.

In the next section, a method of deducing unmixedness from experimental carbon monoxide (CO) measurements is proposed. Like the methods described in Fig. 2 and 3, this technique can be applied to estimate unmixedness in practical LP combustors under fired conditions. Furthermore, the relationship between the experimental data and the perfectly premixed baseline is significantly more simple than that in Fig. 2 and 3.

## CARBON MONOXIDE EMISSIONS FROM LEAN PREMIXED COMBUSTORS

Before discussing the technique for computing unmixedness with combustor CO emissions measurements, the characteristic trends of experimental CO measurements with changing combustor equivalence ratio (chemical kinetics) and residence time (fluid mechanics) are reviewed. Qualitative trends for CO versus main equivalence ratio at two different residence times are shown in Fig. 4. Lower equivalence ratios yield lower flame temperatures in the combustor which do not promote substantial CO oxidation through the CO + OH reaction before quenching occurs. As the mean equivalence ratio is increased, the kinetic time for CO oxidation decreases rapidly, and CO levels approach equilibrium values before quenching occurs. Further increases in equivalence ratio past the intersection of the kinetic and equilibrium regimes ($\phi^*$) leads to higher flame temperatures which promote $CO_2$ dissociation through the $CO_2$ + H reaction and thus higher CO levels. Therefore, CO levels are dominated by oxidation kinetics when the equivalence ratio is less than $\phi^*$ and by equilibrium when greater than or equal to $\phi^*$. Figure 4 also indicates that while the equilibrium CO trend is fixed for a given fuel type, inlet pressure, and inlet temperature of the fuel and air, the kinetic CO curve shifts down as the combustor residence time is increased. Therefore, $\phi^*$ shifts to the left as the combustor residence time is lengthened.

Examples of CO emissions which correspond to the kinetic and CO equilibrium regimes in Fig. 4 have been presented in recent literature. For example, data from the single, quarts–lined burner of Lovett and Mick (1995) are shown in Fig. 5 in the form of an emissions tradeoff plot. On this type of graph, $NO_x$ is proportional to mean equivalence ratio. Inlet conditions are constant along each of the curves shown in Fig. 5. The CO data at the $NO_x$ levels below and above the minimum for each curve correspond to the kinetic and equilibrium regimes in Fig. 4, respectively. Note that in the latter regime, there is no classical $NO_x$/CO trade–off: both emissions increase with increasing premixer mean equivalence ratio. The data which will be focused on here are from the experiments of Joshi et al. (1994).

Joshi et al. used several different test rig configurations to evaluate the Double Annular Counter Rotating Swirler (DACRS) premixer. Tests were performed with natural gas under conditions representative of those in aeroderivative turbines.



Downloaded from http://asmedigitalcollection.asme.org/GT/proceedings-pdf/GT1997/78699/V002T06A008/2409092/v002t06a008-97-gt-073.pdf by guest on 02 December 2022

CO emissions measurements taken from the single cup test rig shown in Fig. 6a are the focus of the work here. The rig was configured with the DACRS II premixer shown in Fig. 6b and an uncooled, high temperature ceramic wall with no air addition sites downstream of the dome exit. Reference velocity was held constant at approximately 12 m/s during testing. Emissions were measured along the combustor centerline with an aero—quench probe designed per guidelines of Roffe and Venkataramani (1978b).

Exhaust plane CO measurements from the 620 K, 5 atm tests were digitised from Joshi et al. (1994) and are shown in Fig. 7, where one low datum believed erroneous is excluded from further analysis here. The remaining data clearly correspond to the equilibrium CO regime in Fig. 4. Furthermore, probe measurements along the combustor axis made by Joshi et al. indicated that CO levels reached an equilibrium state (i.e., the axial gradient of CO concentration approached zero) about 0.1 m downstream of the premixer exit (see Fig. 6a).

The experimental data in Fig. 7 are also compared with the equilibrium COEI computed with STANJAN (Reynolds, 1987) at the fully mixed main equivalence ratio for an assumed natural gas composition (H/C = 3.8). In a combustor where CO reaches equilibrium upstream of the probe location, the measured COEI should correspond to the computed equilibrium COEI. In Fig. 7 the computed COEI curve for pure propane (H/C = 2.7) is used as an upper limit to show that the discrepancy between measured and equilibrium CO cannot be attributed to the assumed fuel type. Similarly, a natural gas preheat temperature of 500 K is used as an upper limit to show that the discrepancy is not due to assumed fuel inlet temperature. Finally, +2% error bars are shown to indicate that the difference is not due to error in the actual versus nominal fuel/air ratio.

Since only the nominal operating conditions and natural gas composition are available for the Joshi et al. data, one must assume that the discrepancy between the measured and equilibrium COEI in Fig. 7 is an indication of unmixedness. It is also thought that the solid computed equilibrium CO curve corresponds most closely to the actual test conditions of Joshi et al. and therefore, this case is taken as the perfectly premixed baseline (s = 0). Nevertheless, the technique of estimating unmixedness from the displacement between measured and equilibrium CO curves for combustors in general will be illustrated with the Joshi et al. data.

## EVALUATING MIXEDNESS WITH CARBON MONOXIDE EMISSIONS MEASUREMENTS

As in the $NO_x$ model discussed above, unmixedness is modeled as a distribution of equivalence ratios associated with the reacting eddies convecting through the combustor. However, in this case, one is concerned with CO emissions that exceed equilibrium values due to unmixedness. Equation (3) is graphed in Fig. 8 along with the baseline equilibrium COEI curve from Fig. 7. As shown in Fig. 8, it is the increase in temperature associated with the richer eddies which leads to the increase in equilibrium CO and thus increased CO emissions, if mean equivalence ratio is greater than $\phi^*$. Equation (3) is used to weight the equilibrium values over the reacting eddies passing through the emissions measurement plane in the combustor to compute the total COEI for any mean equivalence ratio and s:

$$\mathrm{COEI}(\overline{\phi}_m)\big|_{eq,s}=\int_0^{1.4}\Psi(\phi_{eddy})\mathrm{COEI}\big|_{eq}d\phi_{eddy} \quad (6)$$

$(\mathrm{COEI}|_{eq})$ is represented with a piecewise polynomial fit, and the integration limits are selected following the reasoning discussed with respect to Eq. (5).

In order to quantify unmixedness for the data shown in Fig. 7, the s parameter in Eq. (6) is adjusted such that Eq. (6) is equal to the measured CO at each value of mean equivalence ratio. The computed values of s for the Joshi et al. (1994) data in Fig. 7 are shown in Fig. 9. Also presented in Fig. 9, taken from Mello et al. (1997), are data for selected Combustor A run conditions (Barnes et al., 1996; Barnes and Mellor, 1997) and for a third LP combustor, Combustor C, which was tested in the facilities of Solar Turbines (see Mello et al., 1997). Unlike the rig of Joshi et al. (1994), both Combustors A and C are film—cooled. Consequently, Mello et al. (1997) assume equilibrium obtains at the overall equivalence ratio (that is, at the burner outlet temperature) for the CO measured—versus—equilibrium analysis of unmixedness in Combustors A and C.

In contrast to the deduction of s parameter independent of $\phi$ based on the $NO_x$ methodology of Fig. 2, the values of unmixedness parameter for all three combustors presented in Fig. 9 vary inversely with premixer mean equivalence ratio. This observation suggests that mixing is enhanced as the linear momentum of the fuel jets to the air flow in the premixer, that is, the penetration of the fuel jets,



Downloaded from http://asmedigitalcollection.asme.org/GT/proceedings-pdf/GT1997/78699/V002T06A008/2409092/v002t06a008-97-gt-073.pdf by guest on 02 December 2022

is increased. Additionally, the results in Fig. 9 imply a strong influence of premixer design with a weaker effect of air inlet conditions on unmixedness, very desirable trends indeed. Mello et al. (1997) analyse the Combustor A and C data in more depth, as well as present a direct comparison of s parameters for these two combustors deduced from both $NO_x$ and CO emissions measurements.

## CONCLUSIONS

The principal advantages of deducing unmixedness for a given set of LP combustor data from CO measurements over current techniques are:

(1) Low Cost. Unmixedness can be measured during fired combustor rig tests via standard emissions measurement instrumentation.

(2) Non–Intrusive. The fluid mechanics and chemical kinetics associated with CO oxidation and CO equilibrium in the LP combustor are not affected by exhaust plane probe measurements.

(3) Adaptive. The method can be applied to a rig configured with a single or multiple premixer nozzles.

However, application of the technique is subject to some constraints:

(1) $\overline{\phi}_m \geq \phi^*$. Recalling the trends shown in Fig. 4, the technique can only be applied to estimate unmixedness for operating conditions in the CO equilibrium regime above $\phi^*$. This condition typically does not apply to nominal, full power LP combustor operating conditions. Therefore, in practice it is likely that estimates of unmixedness for operating conditions below $\phi^*$ will have to be extrapolated from unmixedness measurements above $\phi^*$, and from idle to full load conditions. This issue can be addressed only via future experimental work.

(2) Little or no air flow other than that through the premixer. In addition to the data of Joshi et al. (1995) and Lovett and Mick (1995), other examples of LP CO equilibrium data taken from flameholder and combustor rigs above $\phi^*$ include Snyder et al. (1994a) and Puri et al. (1995). However, in order to perform the unmixedness analysis with the CO measurements, the temperature associated with equilibrium must be easily defined. In the case of the Joshi et al. (1994) tests (see also Snyder et al., 1994a), the rig was configured with a ceramic liner with no air addition downstream of the premixer exit plane (i.e., 100% of the combustor air flow passed through the LP flame). Thus, the premixer flame temperature at the mean equivalence ratio is used to characterise the thermal environment in which equilibrium obtains in the combustor. If air is added through film cooling slots or dilution holes (such as in Combustors A and C, data for which are shown in Fig. 9, and the rigs of Lovett and Mick, 1995 and Puri et al., 1995), the temperature associated with CO equilibrium may be closer to that at the burner outlet. In this case, even for s greater than zero, equilibrium CO levels may be below (<< 1 ppmvd) the accuracy of CO instrumentation (see Barnes et al., 1996 and Mello et al., 1997). Therefore, the ideal combustor configuration for use with the CO unmixedness method is a premixer attached to a ceramic, nearly adiabatic combustor liner with no film cooling slots or dilution holes (e.g., those of Joshi et al., 1994 and Snyder et al., 1994a). For a LP combustor, such a liner is a necessity because it allows for more efficient use of combustor air flow to reduce the premixed flame temperature and LP $NO_x$. These observations indicate that constraint (2) is consistent with state–of–the–art LP technology.

(3) Adequate quenching of CO reactions in the sampling rake or probe. Failure to freeze the CO chemistry at combustor conditions will lead to incorrect conclusions regarding premixer performance.

If LP CO data are measured in a practical combustor rig which satisfies the operating constraints listed above, the premixer designer should observe the qualitative equilibrium trends indicated in Fig. 10. This graph is analogous to that shown in Fig. 3; however, it is believed that unmixedness is the only variable between the baseline equilibrium curve and the measured curves at a given premixed mean flame temperature. Therefore, accurate estimates of s should be possible following Eq. (6).

## ACKNOWLEDGEMENTS

This paper was prepared with the support of the U. S. Department of Energy, Morgantown Energy Technology Center, under cooperative agreement No. DE–FC21–92MC29061. L.P. Golan and D. Fant of the advanced Gas Turbine systems Research Program at the South Carolina Energy R&D Center served as technical monitors.

## REFERENCES

Agarwal, Y., Hadeishi, T. and Robben, F. (1976), "Measurement of $NO_2$ concentration in combustion using fluorescence excited by an argon–ion laser,"



Downloaded from http://asmedigitalcollection.asme.org/GT/proceedings-pdf/GT1997/78699/V002T06A008/2409092/v002t06a008-97-gt-073.pdf by guest on 02 December 2022

AIAA Paper No. 76—136.

Barnes, J.C., Mello, J.P., Mellor, A.M. and Malte, P.C. (1996), "Preliminary study of $NO_x$, CO, and lean blowoff in a piloted—lean premixed combustor. Part I: experimental; part II: modeling," 1996 Technical Meeting, Central States Section/The Combustion Institute.

Barnes, J.C. and Mellor, A.M. (1997), "Effects of unmixedness in piloted—lean premixed gas turbine combustors," ASME Paper No. 97—GT—???.

Fletcher, R.S. and Heywood, J.B. (1971), "A model for nitric oxide emissions from aircraft gas turbine engines," AIAA Paper No. 71—123.

Fric, T.F. (1993), "Effects of fuel—air unmixedness on $NO_x$ emissions," AIAA J. Propuls. Power 9, 708—713.

Gulati, A. and Warren, R.E. (1994), "$NO_2$—based laser—induced fluorescence technique to measure cold—flow mixing," AIAA J. Propuls. Power 10, 54—61.

Hautman, D.J., Haas, R.J. and Chiappetta, L. (1991), "Transverse gaseous injection into subsonic air flows," AIAA Paper No. 91—0576.

Jones, W.P. and Launder, B.E. (1972), "The prediction of laminarisation with a 2—equation model of turbulence," Int. J. Heat Mass Transfer 15, 301—312.

Joshi, N.D., Epstein, M.J., Durlack, S., Marakovits, S. and Sabla, P.E. (1994), "Development of a fuel/air premixer for aero—derivative dry low emissions combustors," ASME Paper No. 94—GT—253.

Leonard, G. and Stegmaier, J. (1994), "Development of an aeroderivative gas turbine dry low emissions combustion system," Trans. ASME 116, 542—546.

Lovett, J.A. and Mick, W.J. (1995), "Development of a swirl and bluff—body stabilised burner for low—$NO_x$, lean—premixed combustion," ASME Paper No. 95—GT—166.

Magruder, T.D., McDonald, J.P., Mellor, A.M., Tonouchi, J.H., Nicol, D.G. and Malte, P.C. (1995), "Engineering analysis for lean premixed combustor design," AIAA Paper No. 95—3136.

Mello, J.P, Mellor, A.M., Steele, R.C. and Smith, K.O. (1997), "Predicting unmixedness in lean premixed turbine combustors," Submitted to AIAA Joint Propulsion Conference.

Mikus, T. and Heywood, J.B. (1971), "The automotive gas turbine and nitric oxide emissions," Comb. Sci. Tech. 4, 149—158.

Mongia, R., Tomita, E., Hsu, F., Talbot, L. and Dibble, R. (1996), "Optical probe for in—situ measurements of air—to—fuel ratio in low emission engines," AIAA Paper No. 96—0174.

Puri, R., Stansel, D.M., Smith, D.A. and Rasdan, M.K. (1995), "Dry ultra—low $NO_x$ 'Green Thumb' combustor for Allison's 501—K series industrial engines," ASME Paper No. 95—GT—406.

Rasdan, M.K., McLeroy, J.T. and Weaver, W.E. (1994), "Retrofittable dry low emissions combustor for 501—K industrial gas turbine engines," ASME Paper No. 94—GT—439.

Reynolds, W.C. (1987), "STANJAN Version 3.93," Dept. of Mech. Eng., Stanford Univ.

Roffe, G. and Venkataramani, K.S. (1978a), "Experimental study of the effects of flameholder geometry on emissions and performance of lean premixed combustors," NASA CR—135424.

Roffe, G. and Venkataramani, K.S. (1978b), "Emissions measurements for a lean premixed propane/air system at pressures up to 30 atmospheres," NASA CR—159421.

Snyder, T.S., Rosfjord, T.J., McVey, J.B., Hu, A.S. and Schlein, B.C. (1994a), "Emissions and performance of a lean—premixed gas fuel injection system for aeroderivative gas turbines engines," ASME Paper No. 94—GT—234.

Snyder, T.S., Rosfjord, T.J., McVey, J.B. and Chiappetta, L.M. (1994b), "Comparison of liquid fuel/air mixing and $NO_x$ emissions for a tangential entry nozzle," ASME Paper No. 94—GT—283.



Downloaded from http://asmedigitalcollection.asme.org/GT/proceedings-pdf/GT1997/78699/V002T06A008/2409092/v002t06a008-97-gt-073.pdf by guest on 02 December 2022

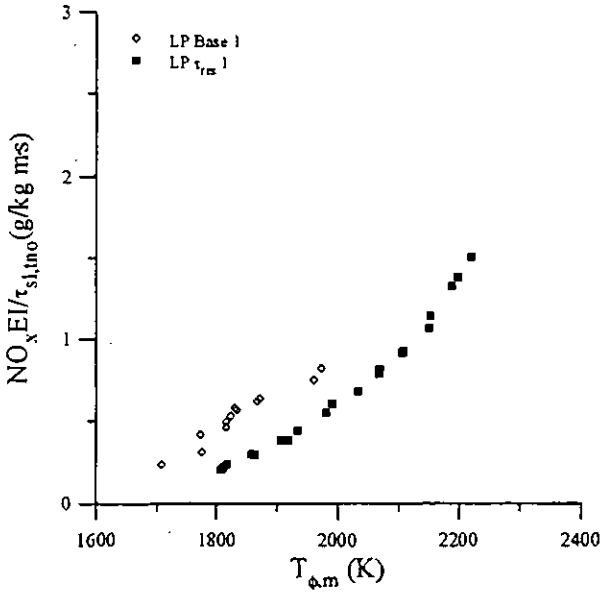


Figure 1. Graph of Combustor A LP $NO_X$ data divided by corresponding $NO_X$ fluid mechanic times ($\tau_{sl,tno}$). The open diamonds represent data obtained at a longer residence time than the closed squares. Inlet temperature and pressure are constant. The fact that the curves do not collapse indicates that unmixedness (s) is a variable between the two datum sets.

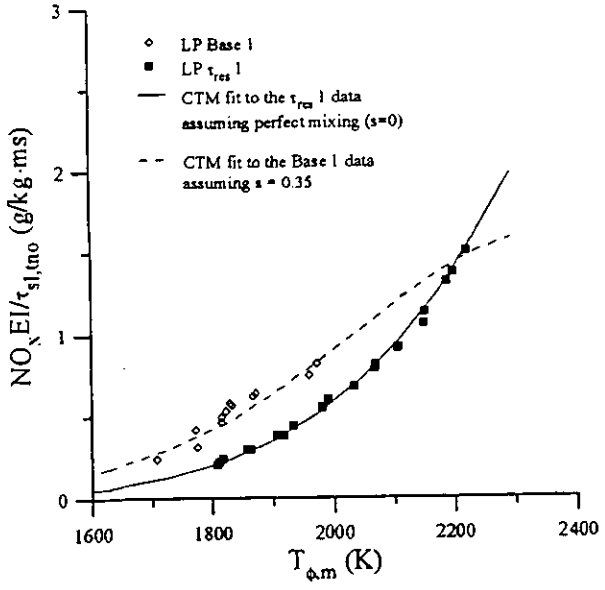


Figure 2. Using the best fit through the LP $\tau_{res}$ 1 data for the perfectly premixed baseline in Eq. (1), s is adjusted such that the LP $\tau_{res}$ 1 best fit correlates the LP Base 1 data. The value of s corresponding to the LP Base 1 data is estimated to be 0.35.

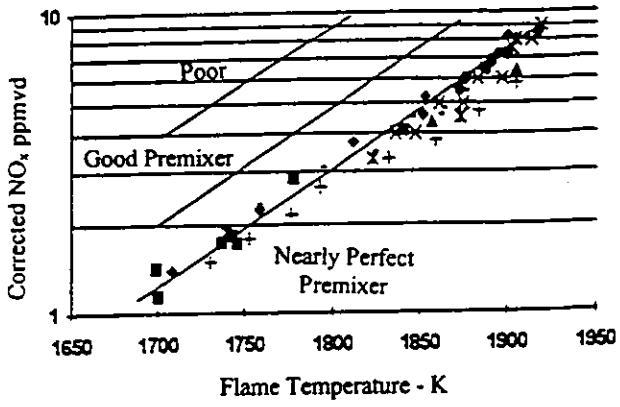


Figure 3. Schematic showing the best fit through the Leonard and Stegmaier (1994) data. The Leonard and Stegmaier best fit is used as the perfectly premixed (s = 0) baseline in this case. The other two other example trendlines correspond to experimental data with s greater than zero (from Leonard and Stegmaier, 1994).

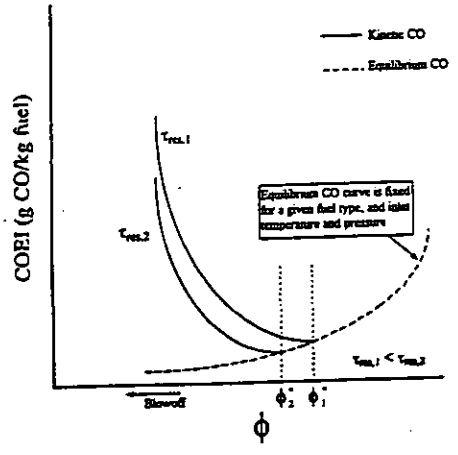


Figure 4. Qualitative trends in LP combustor CO emissions versus mean premixer equivalence ratio for two different residence times ($\tau_{res,1}$ and $\tau_{res,2}$). Fuel type, inlet pressure, and inlet fuel and air temperature are constant. The dashed lines through the intersections of the kinetic and equilibrium CO curves separate the two regimes of CO chemistry. For each respective residence time, $\phi^*$ delineates the regime where the reaction CO + OH limits the oxidation of CO, on the left, from the equilibrium regime on the right.



Downloaded from http://asmedigitalcollection.asme.org/GT/proceedings-pdf/GT1997/78699/V002T06A008/2409092/v002t06a008-97-gt-073.pdf by guest on 02 December 2022

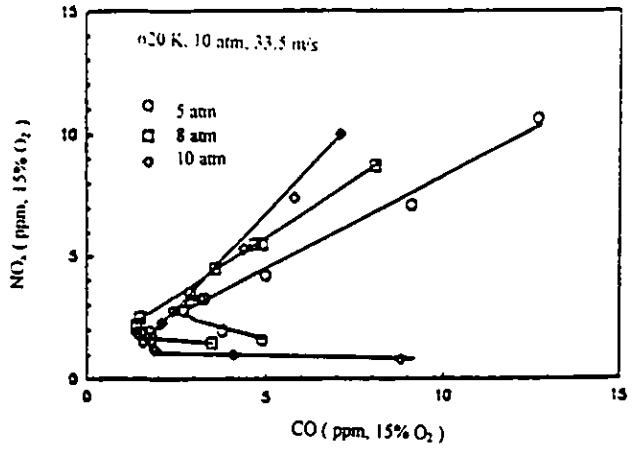


Figure 5. Experimental CO and $NO_x$ data of Lovett and Mick (1995) shown on an emissions tradeoff plot. On this type of graph $NO_x \sim \phi$. Regions of kinetic and equilibrium CO (see Fig. 4) are apparent. The operating conditions shown in the upper left hand corner of the graph should read "620 K, 33.5 m/s"; "10 atm" is a typographical error.

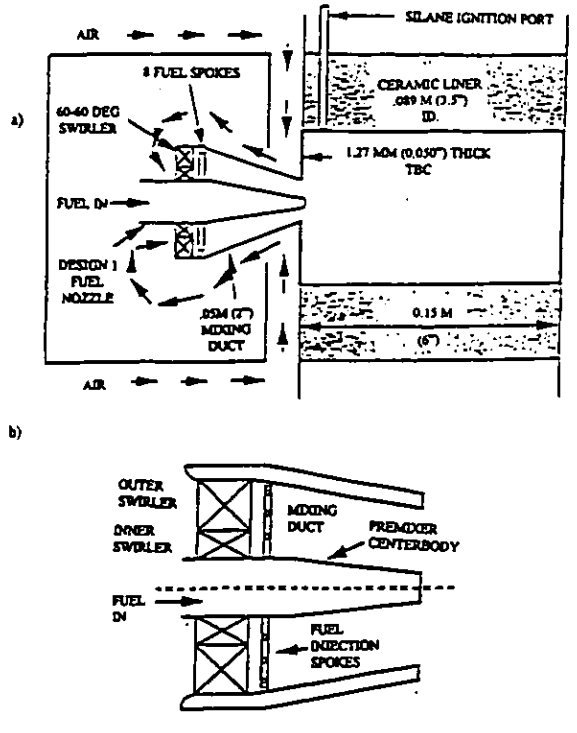


Figure 6. a) Single cup test combustor cross section; b) DACRS II premixer cross section (Joshi et al., 1994).

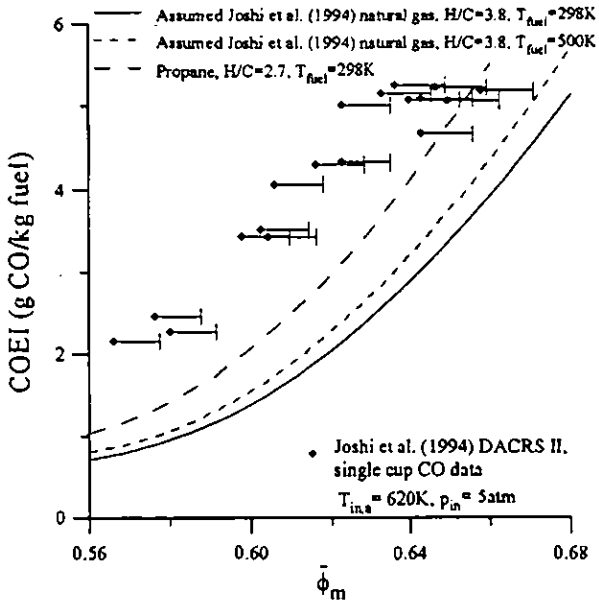


Figure 7. Digitised CO data of Joshi et al. (1994) for $T_{in}$ = 620 K, $p_{in}$ = 5 atm, and constant reference velocity. The propane equilibrium curve is used as an upper limit to show that the discrepancy between measured and equilibrium CO cannot be attributed to the assumed natural gas composition. A natural gas preheat temperature of 500 K is used as an upper limit to show that the discrepancy is not due to assumed fuel inlet temperature. +2% error bars are shown to indicate that the difference is not due to error in the fuel/air measurement.

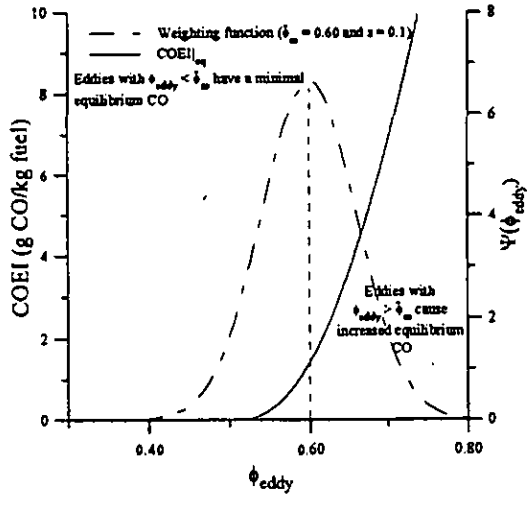


Figure 8. Graph indicating the relationship between a typical Gaussian eddy equivalence ratio distribution and the equilibrium CO curve for the inlet conditions of the data in Fig. 7.



Downloaded from http://asmedigitalcollection.asme.org/GT/proceedings-pdf/GT1997/78699/V002T06A008/2409092/v002t06a008-97-gt-073.pdf by guest on 02 December 2022

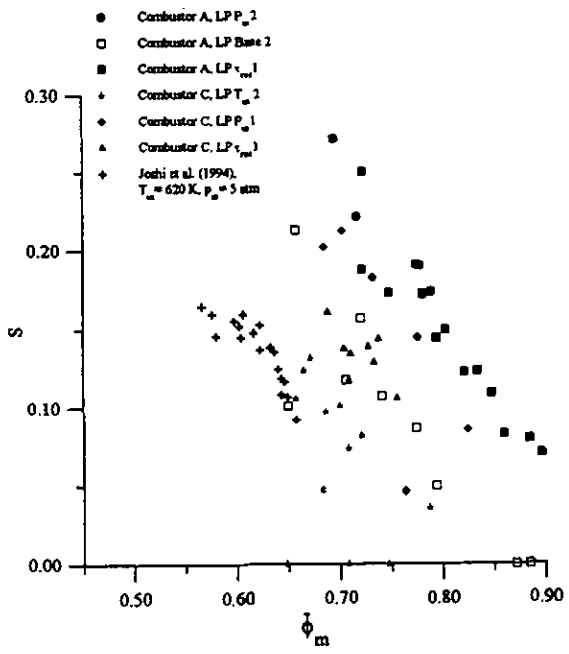


Figure 9. Unmixedness levels deduced from CO emissions (Eq. 6) for the 620 K, 5 atm tests of Joshi et al. (1994) shown in Fig. 7 and for selected Combustor A and C (see text) operating conditions (from Mello et al., 1997).

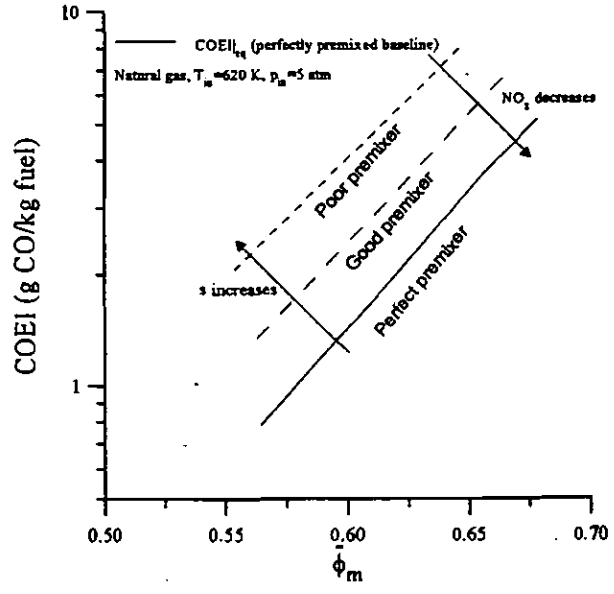


Figure 10. Expected trends in measured COEI with s for mean equivalence ratio greater than $\phi^*$. The baseline case corresponds to equilibrium at $s = 0$.



Downloaded from http://asmedigitalcollection.asme.org/GT/proceedings-pdf/GT1997/78699/V002T06A008/2409092/v002t06a008-97-gt-073.pdf by guest on 02 December 2022